Original Article
Induction of intervertebral disc degeneration using annular puncture and establishment of a disc-safe injection method in a rabbit model using an ultrasound-guided percutaneous approach

Qingxin Song[1*], Meng Li[2*], Junfeng Hong[3*], Yixing Tang[1], Fan Zhang[1], Zhi Chen[5], Canglong Hou[1], Yifeng Wang[1], Songqin Gao[4], Kun Wang[1], Hongxing Shen[1,5]

[1]Department of Orthopedics, Changhai Hospital, Second Military Medical University, Shanghai 200433, People's Republic of China; [2]Department of Ultrasound, Obstetrics and Gynecology Hospital, Fudan University, Shanghai 200090, People's Republic of China; [3]Department of Ultrosound, Fuzhou General Hospital (Dongfang Hospital), Xiamen University, Fuzhou 350025, Fujian, People's Republic of China; [4]Department of Nursing, Changhai Hospital, Second Military Medical University, Shanghai 200433, People's Republic of China; [5]Department of Orthopedics, Renji Hospital, Shanghai Jiao Tong University School of Medicine, Shanghai 200433, People's Republic of China. *Equal contributors.

Abstract: The rabbit annular puncture model of intervertebral disc degeneration (IDD) is among the most widely used models of IDD. We aimed to establish a rabbit model of IDD using a direct, minimally invasive procedure, and to establish a safe approach for disc injection of therapeutic agents. The rabbit model of IDD was established using ultrasound-guided percutaneous annular puncture: 18G to induce disc injury (18G segments), and 27G to evaluate the feasibility and safety of disc injection (27G segments). X-rays, histology and magnetic resonance imaging (MRI) were performed to assess IDD at 4, 8 and 12 weeks after modeling. Disc morphologic changes (by MRI, X-rays and histology), and collagen I and II immunohistochemistry were used to assess IDD. Disc space narrowing was observed as early as 4 weeks and osteophytes were formed at 12 weeks after puncture in the 18G segments, but no such changes occurred in the 27G and control segments. MRI demonstrated a progressive loss of T2WI signal intensity at the 18G segment throughout the 12-week period, while the 27G segment showed only a slight decrease of T2WI signal intensity throughout the 12-week period. Immunohistochemistry showed a progressive loss of the normal architecture and collagens in the 18G segment from 4 to 12 weeks, while the 18G segment showed only a slight change in architecture. These results indicated that using ultrasound-guided percutaneous annular puncture in rabbits; a 27G needle was small enough prevent the induction of IDD and could be a promising method of delivering therapeutic agents into discs.

Keywords: Intervertebral disc disease, rabbit model, ultrasound guidance, puncture, injection

Introduction

Intervertebral disc degeneration (IDD) is a common orthopedic disease that often causes other spinal-related diseases (such as herniation, cauda equine syndrome, lumbar spinal stenosis and degenerative spondylosis) and seriously hinders patient quality of life. The pathophysiology and pathogenesis of IDD are not clearly understood [1].

To study the underlying mechanisms of IDD and its associated systemic biomechanical and biochemical response, various experimental animal models (mini pigs, dogs, goats, monkeys and sheep) have been developed to mimic the pathophysiological changes typically observed in patients with IDD [2-5]. Different methods have been reported for inducing the disease (such as injection and aspiration) [6-8], using different approaches to the disc (invasive, fluoroscopy-guided or computed tomography (CT)-guided) [9-11]. Among these methods, stabbing the disc with a needle using the posterolateral retroperitoneal approach has the advantage to be very appropriate for IDD induction because it reproduces the slow and spontaneous process occurring in most humans. Indeed, focal
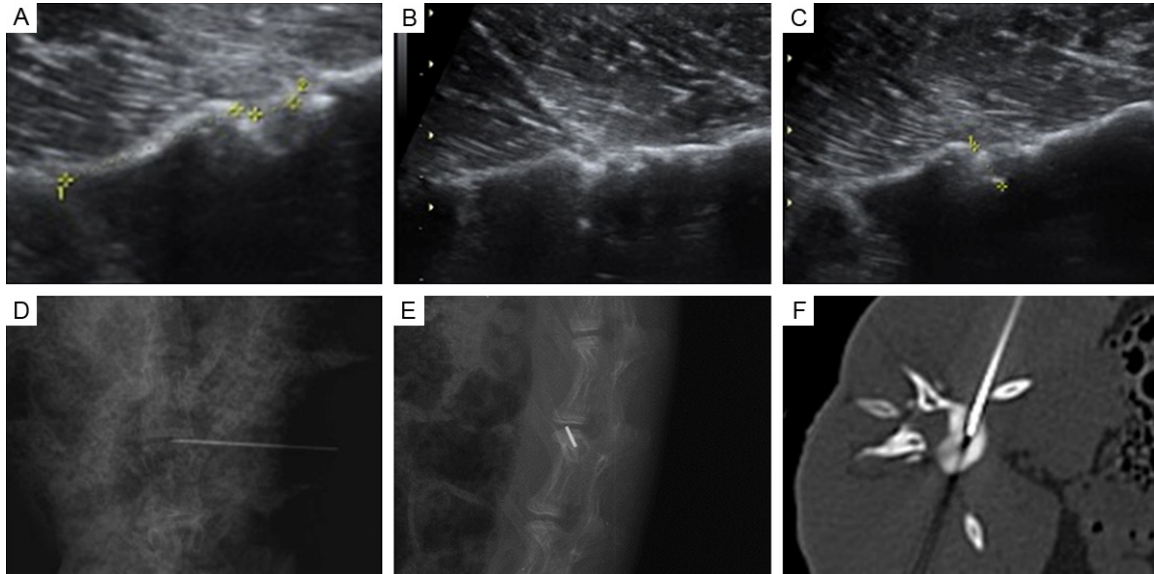
Figure 1. Detailed procedures of US-guided percutaneous puncture technique. A. Identification of the vertebral body and intervertebral disc, showing that the DH was 2.5 mm (arrow). B. The procedure was paused when the needle pinpoint touched the rim of the disc. C. The pinpoint of the needle was stabbed into the nucleus pulposus for about 5 mm according to US. D and E. The orientation and position of the needle were verifying by sagittal and lateral CT scans. F. CT scan verified the position and length of the needle insertion.

annular injury has been shown to be an initiator of IDD induced by needle puncture. Since the development of the stab injury model [12-14], it has become one of the most widely used and realistic models for investigating changes in the morphological, mechanical and biochemical properties during IDD, and its mild degeneration is suitable to evaluate biologic therapies.

A possible treatment of IDD would be direct delivery of specific growth factors, adenovirus particles or autologous cells directly into the discs [15-17]. Therefore, determining the safe needle size, number of punctures and technique is an important issue to prevent causing more harms than goods to the discs [18]. In addition, an ultrasound (US)-guided approach could be easier to perform in most clinical settings compared with the open, fluoroscopy-guided and CT-guided approaches that require extensive and expensive equipment and personnel.

Therefore, the aim of the present study was to establish a rabbit model of IDD using a direct minimally invasive procedure, and to establish a safe approach for disc injection of drugs. Results of the present study could be used to design new approaches to deliver therapeutic

agents to intervertebral discs without further damaging them.

Materials and methods

Rabbits and study design

The Animal Care and Use Committee of the Second Military Medical University approved all animal experimental protocols, which followed the principles of laboratory animal care (NIH publication No. 85-23, revised 1985) and the current version of the Chinese Law on the Protection of Animals. Eighteen New Zealand white rabbits (Experimental animal center of Second Military Medical University, Shanghai, China) weighing 2.5-3.0 kg underwent percutaneous annular puncture under US guidance. The rabbits were then followed up by X-rays and magnetic resonance imaging (MRI) at 4, 8, and 12 weeks after surgery. At each time point, six rabbits were chosen randomly, anesthetized with pentobarbital sodium (0.15 mL/kg intravenously) and then killed with an intravenous delivery of 5 mL of 3% sodium pentobarbital. The intervertebral disc was harvested using a posterolateral retroperitoneal approach for histological analysis. All motion segments, including L2-3, L3-L4, L4-L5, and L5-L6 were
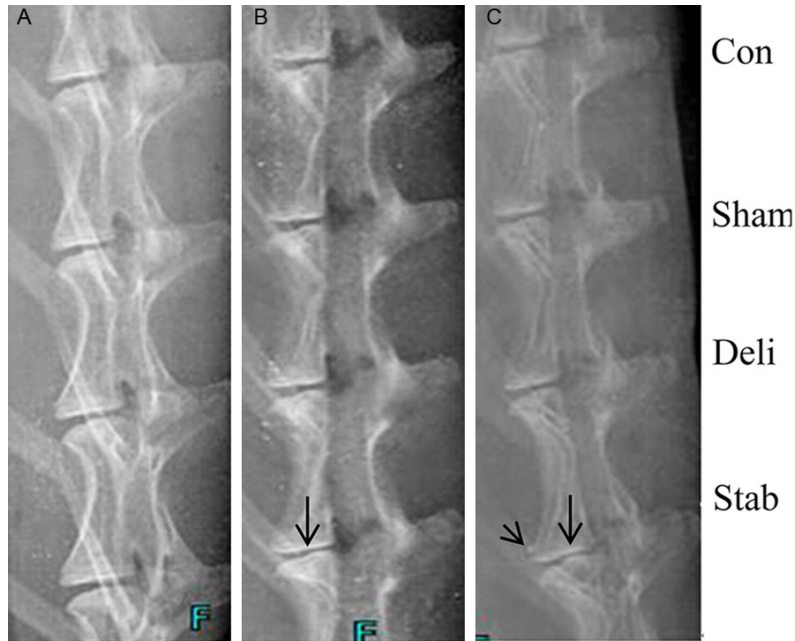
Figure 2. Representative changes in X-rays at 4, 8, and 12 weeks postoperatively. A. Mild endplate calcifications and disc space narrowing in 18G segments at 4 weeks. B. Prominent disc space narrowing and midrate endplate calcifications were present at 8 weeks postoperatively. C. Prominent wedging, endplate calcifications and subchondral sclerosis were seen (arrow), with osteophyte being present on disc margin with disc space narrowing.

(the needle did puncture the skin, but not the disc). The puncture procedure was controlled manually and paused when the needle pinpoint touched the rim of the disc. The pinpoint of the needle was stabbed into the nucleus pulposus for about 5 mm (**Figure 1C**).

After puncture, an X-ray and CT scan were conducted to confirm the puncture position of the needle (**Figure 1D-F**). Also small amount of nucleus pulposus in the canal of the needle was carefully examined to ensure that he needle had correctly stabbed into the nucleus pulposus. The puncture was performed in triplicate.

MRI

harvested and stored in 10% neutral-buffered formalin.

US-guided annular puncture procedures

US-guided annular percutaneous needle puncture was used to establish this model and to assess the efficacy and relative safety of an intradiscal delivery method. First, US was conducted through the retroperitoneal approach to identify the iliac spine and the location of intervertebral discs (**Figure 1A**). Then, target disc was confirmed from the caudal to cephalic spine according to the position of the iliac spine. Once the target disc center was confirmed, punctures with the 18G and 27G needles were then subcutaneously performed separately under US guidance into the disc center (**Figure 1B**). An 18G or 27G needle were penetrated toward the center of the disc under US guidance, and the needle pinpoint was then confirmed to be positioned in the disc center at a depth of 5 mm [19]. L5-L6 segments were injured with the 18G needle to induce IDD. The 27G needle was tested at the L4-L5 position. L2-L3 segments were used as controls. The L3-L4 segment underwent a sham procedure

All lumbar spinal segments were assessed using conventional MRI at 4, 8 and 12 weeks. MRI was acquired using a transmit-receive quadrature knee coil (MAGNETOM Avanton, SIEMENS, Germany). T2WI images in the sagittal plane were obtained. The disc morphologic changes were divided into five categories according to the methods of Pfirrmann et al. [20].

X-ray

Lateral X-rays were obtained from each lumbar spine at 4, 8 and 12 weeks postoperatively. The disc height (DH) was measured from the lateral X-rays. The average disc thickness was calculated by averaging the distance between the endplates at the anterior, middle and posterior portions of the disc. The preoperative X-ray was used for as baseline. The change in DH was expressed as %DH = postoperative DH/preoperative DH*100% [21].

Histology and immunohistochemistry

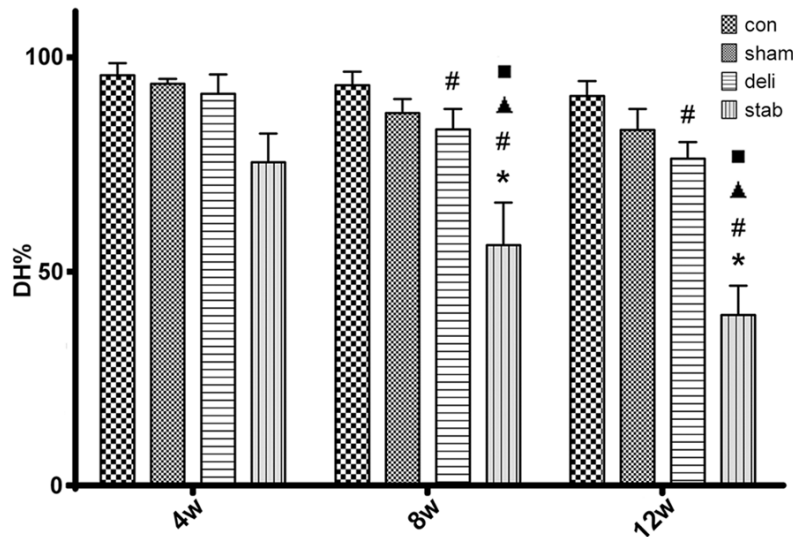One half of the harvested lumbar discs (including the endplates) were sampled and fixed in

Figure 3. Changes in DH at 4, 8 and 12 weeks postoperatively. #$P<0.05$ versus the control segments, *$P<0.05$ versus the sham segments, ■$P<0.05$ versus the sham segments, ▲$P<0.05$ versus the 18G segments at 4 weeks. Data are presented as means ± SD percentage of reduction in DH calculated by three independent observers.
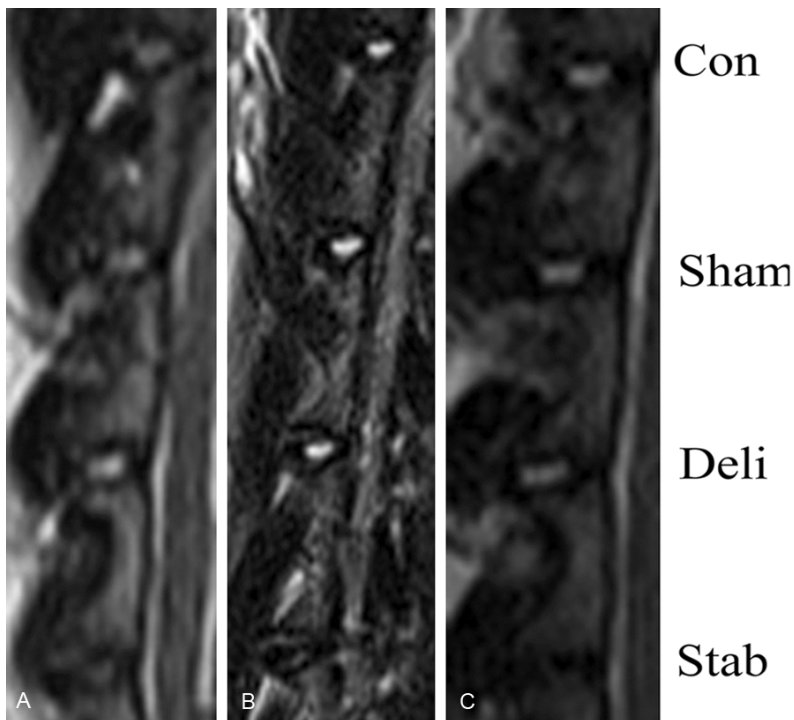

Figure 4. Representative changes in T2WI MRI at 4, 8 and 12 weeks postoperatively. A. Signal intensity of the 18G segments was partially decreased at 4 weeks after stabbing. B. Decreased signal intensity and DH were present at 8 weeks. C. Signal intensity and DH had decreased markedly in 18G segments at 12 weeks.

10% neutral-buffered formalin overnight. The discs were decalcified using ethylenediamine tetraacetic acid. Decalcified discs were serially dehydrated in ethanol and embedded in paraffin. The blocks were cut into 4-μm-thick sections. Hematoxylin-eosin staining was then conducted.

For immunohistochemistry, rabbit polyclonal collagen I and II antibodies (1:100 dilution; Boster, Wuhan, China) were used to evaluate the changes in collagen in the discs using a standard immunoperoxidase method with 3,3-diaminobenzidine tetrachloride dehydrate.

Statistical analysis

Continuous data are presented as means ± standard deviations (SD). One-way analysis of variance with the least squares difference post hoc test was used to assess the differences. SPSS 16.0 (IBM, Armonk, NY, USA) was used for analysis. *P*-values $P<0.05$ were considered significant.

Results

X-ray and MRI

A slight intervertebral disc space narrowing was first observed in the 18G segments at 4 weeks after surgery (75.50% of the preoperative DH, $P<0.05$ vs. preoperative, but 95.83%, 93.83% and 91.50% of the control, sham and 27G segments, respectively, all three $P<0.05$ vs. 18G) (**Figures 2A** and **3**). The reduction in DH at 8 weeks after surgery was more apparent in the 18G segments (56.17% of the preoperative DH, $P<0.05$ vs. preoperative, and 93.50%,
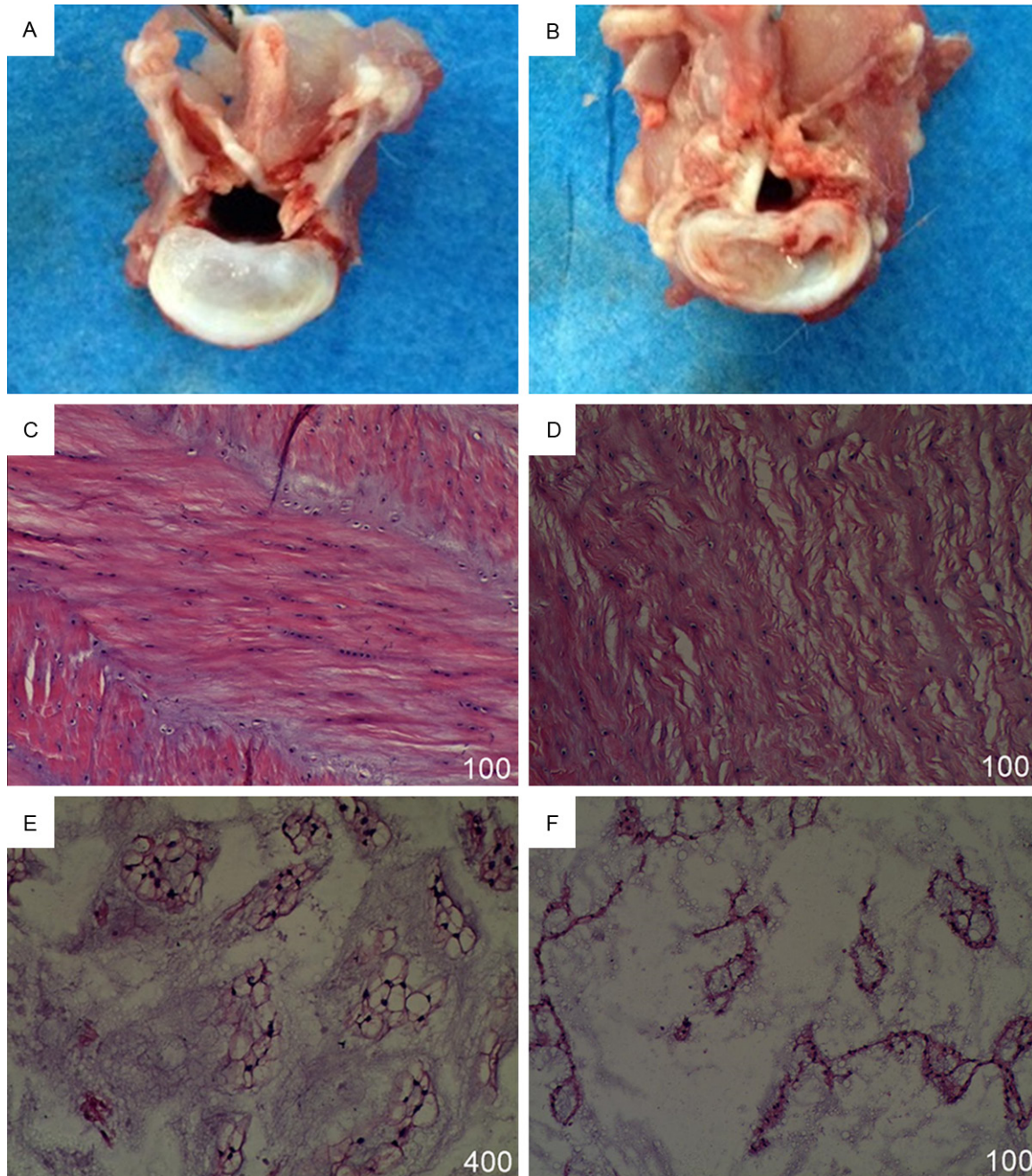
Figure 5. Typical morphologic changes at 4, 8 and 12 weeks after needle puncture. A. Normal disc. Fibrous annulus fibrosus with obvious concentric fibrous lamellae and nucleus pulposus with affluent gel-like structure. B. Moderately degenerated disc. Disorganized fibrous lamellae at annulus fibrosus and decreased water content in nucleus pulposus, with chondroid tissue formed around the needle hole. Fibrocartilage tissue was formed at annulus fibrosus, with osteoid tissue formed around the needle hole with nucleus pulposus fibrosis. Osteoid tissue was formed at annulus fibrosus and nucleus pulposus. C. Hematoxylin-eosin staining of normal disc with concentric fibrous lamellae. D. Hematoxylin-eosin staining of degenerated disc with disorganized lamellae. C and E. Hematoxylin-eosin staining of normal disc, composed of an outer fibrous annulus fibrous with obvious concentric fibrous lamellae and an inner nucleus pulposus with large vacuoles in cells and regular extracellular matrix. F. Hematoxylin-eosin staining of nucleus pulposus of degenerated disc with disorganization of the extracellular matrix. More nucleus pulposus cells with elliptical shape were distributed unevenly owing to ingrowth of proteoglycan matrix into multiple cell islands.

87.12% and 83.17% in the control, sham and 27G segments, respectively, all three P<0.05

vs. 18G) (**Figures 2B** and **3**). At 12 weeks, DH had decreased further in the 18G segments
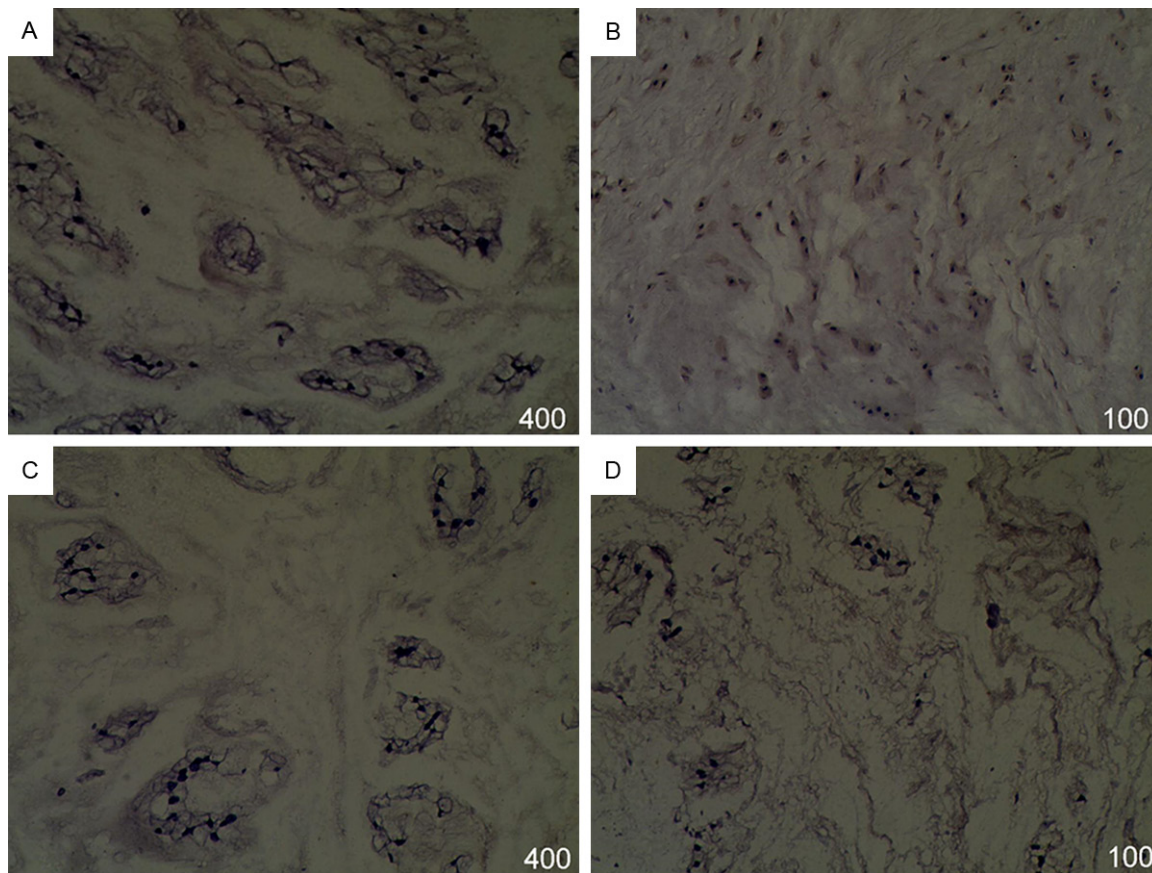
Figure 6. Histological analysis of nucleus pulposus at 12 weeks. Hematoxylin-eosin and immunohistochemistry of normal and degenerated discs. A. Collagen type I immunohistochemistry of normal nucleus pulposus. B. Collagen type I immunohistochemistry of degenerated disc nucleus pulposus. C. Collagen type II immunohistochemistry of normal nucleus pulposus. D. Collagen type II immunohistochemistry of degenerated disc nucleus pulposus.

(39.83% of the preoperative DH, P<0.05 vs. preoperative, and 92.21%, 83.12% and 76.33% in the control, sham and 27G segments, respectively, all three P<0.05 vs. 18G) (**Figures 2C** and **3**). In addition, at 12 weeks, the 18G segments displayed significant anterior and posterior osteophytes and endplate sclerosis (**Figure 2C**). On the other hand, the control, sham and 27G segments did not show these lesions during the 12-week period. In the control, sham and 27G segments, no significant difference was seen in DH (**Figure 3**).

MRI showed that the signal intensity of the nucleus pulposus decreased progressively in the 18G segments during the 12-week postoperative period (**Figure 4A-C**). The 18G segments showed lower signal intensity than the control, sham and 27G segments at each time point (**Figure 4**), with the lowest signal intensity being observed at 12-wk postoperatively

(**Figure 4**). No significant difference was observed in disc condition by MRI between the control, sham and 27G segments at any time point, suggesting the safety of the use of 27G puncture. Using the MRI classification of IDD, grade II degenerative changes were observed in the 18G segments at 4 weeks, while grade III or IV were observed at 8 weeks, and grade IV or V at 12 weeks. The 27G segments showed a slight decrease in the T2WI signal at 12 weeks with grade II degeneration on T2WI. In contrast, the control and sham segments remained relatively constant during the 12-week period, with grade I on T2WI.

Gross morphological and histological analyses

Compared with the control segments at the different time points, the loss of the gel-like nature of the nucleus and brown pigmentation were clearly seen in the 18G segments (**Figure 5B**).

In addition, considerable delamination of the annular layers was present, particularly around the puncture part of the annulus, with no distinct demarcation between the annulus-nucleus borders. These changes were observed in the 18G segments over the entire 12-week period. Ossification and anterior osteophytes formation in the 18G segments were detected at 12 weeks.

Hematoxylin-eosin staining revealed that the normal disc was composed of an outer fibrous annulus fibrous with obvious concentric fibrous lamellae and an inner nucleus pulposus with an amorphous matrix and heterogeneous cells (**Figure 5C** and **5E**). The nucleus pulposus of the 18G segments was characterized by an increase in fibrous tissue and a decrease in volume that included shrinkage or disappearance. More nucleus pulposus cells with an elliptical shape were distributed unevenly owing to ingrowth of proteoglycan matrix into multiple cell islands (**Figure 5F**). The lamellar architecture of the inner, middle, and outer annulus became more disorganized with increasing time after 18G puncture (**Figure 5D**).

Immunohistochemistry

Immunohistochemistry showed that the expression of collagen II was decreased in discs with IDD. In the degenerative nucleus pulposus, a decrease in staining for collagen II was observed (**Figure 6D**), and staining for collagen I was detected in the extracellular matrix (**Figure 6B**). Immunohistochemistry revealed a clear tendency for a more pronounced decrease in the expression of collagen II and an increase in collagen I in the degenerated nucleus pulposus over time.

Discussion

The aim of the present study was to establish a rabbit model of ISS using a direct, minimally invasive procedure, and to establish a safe approach for disc injection of drugs. Results showed that DH was reduced as early as 4 weeks and osteophytes were formed at 12 weeks after puncture in the 18G segments, but no such changes occurred in the 27G segments. MRI demonstrated a progressive loss of T2WI signal intensity at the 18G segments throughout the 12-week period, while the 27G segment showed only a slight decrease of T2WI

signal intensity throughout the 12-week period. Immunohistochemistry showed a progressive loss of the normal architecture in the 18G segments from 4 to 12 weeks, while the 27G segments showed only a slight change in architecture.

The induced disc disorder model is characterized by progressive degeneration, a loss of disc height (DH) and altered biomechanical strength [22]. In the stab injury model, there is a herniation of the nucleus pulposus from the intervertebral disc after needle puncture of the disc annulus, which leads to the loss of the loading pressure that is balanced with the suction pressure in the normal healthy disc. At the onset of a disc disorder, the imbalance between the hydrostatic and osmotic pressures triggers fluid exudation and volume reduction. Subsequently, the disc undergoes a process of remodeling that culminates in IDD. When the stab injury model was created in rodents, it was shown that the morphologic changes in the disc and vertebral body were similar to those seen in IDD in humans [18]. Despite its clinical relevance and widespread use in the field of intervertebral disc research, the major concern with the stab injury model is the perturbations of the physiologic function around the disc. Therefore, in the present study, we designed a new method of creating an IDD model in the rabbit using an US-guided needle puncture and we have demonstrated that using a 27G needle does not induce degenerative changes in DH. Therefore, this could be a suitable method for delivering therapeutic agents into the discs.

The stab injury leads to changes in compression in the annulus and results in a decrease in DH. The endplate is vulnerable to fatigue damage, even with normal physiologic load levels [23], and the nutrient transportation can be affected directly by capillaries of cartilage endplate with fluid movement in and out of the disc [24]. Therefore, disc degeneration can be initiated from the vertebral endplate by mechanical disruption. Discs with Schmorl nodes are defects of the vertebral endplate and are considered to represent the advanced degenerative changes at an earlier age [25]. Disc injuries and endplate sclerosis can block nutrient supplement, and the decreased nutrient supplement inhibits matrix synthesis [26]. In the present study, evidence from the X-rays demon-

strated that the DH decreased as the endplate sclerosis occurred. The sclerotization of the stabbed disc endplate was detected at 8 weeks and was obvious at 12 weeks. The stab injury model induces considerable changes to the nucleus, particularly in the biomechanical properties of degenerative discs [27-29]. In the present study, the changes observed after stabbing were consistent with those occurring in human IDD. Radiographically, human IDD is characterized by a reduction in DH [30] and the formation of prominent and, in some cases, bridging osteophytes [31].

A previous investigation have revealed that MRI could be reliable for examination of gross disc morphology [32]. It was reported that the concordance of the classification system with the morphologic and MRI changes was high. Modic et al. [33] reported that the signal loss of the disc on T2WI MRI correlated with the progressive degenerative changes in the intervertebral disc. The relationship between the disc signal intensity on MRI and biochemical changes has also been studied. Indeed, Pearce et al. [34] have shown that the brightness of the nucleus (i.e., the response of the high-signal intensity on T2WI MRI) correlated directly with the proteoglycan concentration but not with the water or collagen content. In the present study, MRI has been used to assess disc degeneration in vivo. The signal intensity of the 18G segments was lower than that of the control, sham and 27G segments, and decreased consecutively from 4 to 12 weeks on T2WI MRI.

Proteoglycans and water are the major components of the normal nucleus. Decreases in their concentrations are considered to be the principal biochemical markers of aging and IDD in humans [35]. Many studies have suggested that IDD is associated with decreased hydration, especially in the nucleus pulposus [36-38]. With IDD, reductions in proteoglycan content and water are most commonly observed in the nucleus, similar to the observations from animal models. Another factor that influences the concentration of proteoglycan is the hydrostatic pressure, which directly affects matrix expression and extracellular matrix synthesis in the intervertebral disc [39]. Reductions in proteoglycan and water content result in a consecutive decline in hydrostatic pressure inside the degenerated disc, and abnormal static pressure greater or lower than physiologic levels

can act catabolically, inhibiting proteoglycan synthesis. In the present study, we punctured the disc and extracted part of the nucleus pulposus. In addition to their water-binding function, small proteoglycans have the ability to bind to collagens, growth factors, and other matrix components [40]. In the present study, it has been shown that collagen II expression in the 18G segments was reduced compared with that in the control and sham segments and decreased consecutively with time. Biochemically, human IDD is characterized by decreased expression of large proteoglycans, such as aggrecan shifts in the collagen expression and changes in collagen cross-linking indicative of increased matrix turnover [41, 42].

The minimally invasive stab model has several advantages for disc degeneration studies at the molecular and animal levels. First, the present model is based on an action that depletes the interference of the paravertebral muscles and ligaments to the disc, rather than the damage effect of the paravertebral muscles and ligaments on the disc, with questionable physiologic relevance to IDD [43]. This is a major advantage compared with scalpel incision into the anterior annulus to initiate a degenerative process. In the present study, an US-guided approach was successful in establishing all models. Indeed, an US-guided approach could be easier to perform in most clinical settings compared with the open, fluoroscopy-guided and CT-guided approaches that require extensive and expensive equipment. This approach would be easy to implement in the clinic when injecting therapeutic agents into a disc [6, 44-46]. Of course, the results of the present study were obtained using an animal model, and further studies are necessary before using this approach in humans.

In conclusion, using ultrasound-guided percutaneous annular puncture in rabbits, a 27G was small enough prevent the induction of IDD and could be a promising method of delivering therapeutic agents into discs. This approach could be used for studying therapeutic agent delivery to the discs without aggravating the discs' condition.

Acknowledgements

81550006), and the The new hundred talents program of Shanghai municipal commission of Health and Family Planning (Grant No. XBR2013099).

Disclosure of conflict of interest

None.

Address correspondence to: Dr. Hongxing Shen, Department of Orthopedics, Changhai Hospital, Second Military Medical University, Shanghai 200433, People's Republic of China. Tel: +86-13524583474; Fax: +86-21-31161584; E-mail: shenhxsci@sina.com

References

[1] Rodrigues-Pinto R, Richardson SM and Hoyland JA. An understanding of intervertebral disc development, maturation and cell phenotype provides clues to direct cell-based tissue regeneration therapies for disc degeneration. Eur Spine J 2014; 23: 1803-1814.

[2] Detiger SE, Holewijn RM, Hoogendoorn RJ, van Royen BJ, Helder MN, Berger FH, Kuijer JP and Smit TH. MRI T2* mapping correlates with biochemistry and histology in intervertebral disc degeneration in a large animal model. Eur Spine J 2014; 24: 1935-1943.

[3] Detiger SE, Hoogendoorn RJ, van der Veen AJ, van Royen BJ, Helder MN, Koenderink GH and Smit TH. Biomechanical and rheological characterization of mild intervertebral disc degeneration in a large animal model. J Orthop Res 2013; 31: 703-709.

[4] Bergknut N, Rutges JP, Kranenburg HJ, Smolders LA, Hagman R, Smidt HJ, Lagerstedt AS, Penning LC, Voorhout G, Hazewinkel HA, Grinwis GC, Creemers LB, Meij BP and Dhert WJ. The dog as an animal model for intervertebral disc degeneration? Spine (Phila Pa 1976) 2012; 37: 351-358.

[5] Lotz JC. Animal models of intervertebral disc degeneration: lessons learned. Spine (Phila Pa 1976) 2004; 29: 2742-2750.

[6] Leckie SK, Bechara BP, Hartman RA, Sowa GA, Woods BI, Coelho JP, Witt WT, Dong QD, Bowman BW, Bell KM, Vo NV, Wang B and Kang JD. Injection of AAV2-BMP2 and AAV2-TIMP1 into the nucleus pulposus slows the course of intervertebral disc degeneration in an in vivo rabbit model. Spine J 2012; 12: 7-20.

[7] Roberts S, Menage J, Sivan S and Urban JP. Bovine explant model of degeneration of the intervertebral disc. BMC Musculoskelet Disord 2008; 9: 24.

[8] Unglaub F, Guehring T, Omlor G, Lorenz H, Carstens C and Kroeber MW. [Controlled distraction as a therapeutic option in moderate degeneration of the intervertebral disc--an in vivo study in the rabbit-spine model]. Z Orthop Ihre Grenzgeb 2006; 144: 68-73.

[9] Cui YN, Zhou RP, Mai QG, Lu M, Xu S, Wang L, Li SL and Jin DD. [Establishment of a rabbit model of lumbar intervertebral disc degeneration via the paraspinal approach]. Nan Fang Yi Ke Da Xue Xue Bao 2012; 32: 404-408.

[10] Yoon SH, Miyazaki M, Hong SW, Tow B, Morishita Y, Hu M, Ahn SJ and Wang JC. A porcine model of intervertebral disc degeneration induced by annular injury characterized with magnetic resonance imaging and histopathological findings. Laboratory investigation. J Neurosurg Spine 2008; 8: 450-457.

[11] Moss IL, Zhang Y, Shi P, Chee A, Piel MJ and An HS. Retroperitoneal approach to the intervertebral disc for the annular puncture model of intervertebral disc degeneration in the rabbit. Spine J 2013; 13: 229-234.

[12] Ford LT and Key JA. The experimental production of intervertebral disc lesions by chemical injury. Surg Forum 1951; 447-453.

[13] Key JA and Ford LT. Experimental intervertebral-disc lesions. J Bone Joint Surg Am 1948; 30A: 621-630.

[14] Smith JW and Walmsley R. Experimental incision of the intervertebral disc. J Bone Joint Surg Br 1951; 33-B: 612-625.

[15] Sobajima S, Vadala G, Shimer A, Kim JS, Gilbertson LG and Kang JD. Feasibility of a stem cell therapy for intervertebral disc degeneration. Spine J 2008; 8: 888-896.

[16] Masuda K. Biological repair of the degenerated intervertebral disc by the injection of growth factors. Eur Spine J 2008; 17 Suppl 4: 441-451.

[17] Bach FC, Willems N, Penning LC, Ito K, Meij BP and Tryfonidou MA. Potential regenerative treatment strategies for intervertebral disc degeneration in dogs. BMC Vet Res 2014; 10: 3.

[18] Martin JT, Gorth DJ, Beattie EE, Harfe BD, Smith LJ and Elliott DM. Needle puncture injury causes acute and long-term mechanical deficiency in a mouse model of intervertebral disc degeneration. J Orthop Res 2013; 31: 1276-1282.

[19] Kong MH, Do DH, Miyazaki M, Wei F, Yoon SH and Wang JC. Rabbit Model for in vivo Study of Intervertebral Disc Degeneration and Regeneration. J Korean Neurosurg Soc 2008; 44: 327-333.

[20] Pfirrmann CW, Metzdorf A, Zanetti M, Hodler J and Boos N. Magnetic resonance classification of lumbar intervertebral disc degeneration. Spine (Phila Pa 1976) 2001; 26: 1873-1878.

[21] Zhou H, Hou S, Shang W, Wu W, Cheng Y, Mei F and Peng B. A new in vivo animal model to cre-

ate intervertebral disc degeneration characterized by MRI, radiography, CT/discogram, biochemistry, and histology. Spine (Phila Pa 1976) 2007; 32: 864-872.

[22] Larson JW 3rd, Levicoff EA, Gilbertson LG and Kang JD. Biologic modification of animal models of intervertebral disc degeneration. J Bone Joint Surg Am 2006; 88 Suppl 2: 83-87.

[23] O'Connell GD, Vresilovic EJ and Elliott DM. Human intervertebral disc internal strain in compression: the effect of disc region, loading position, and degeneration. J Orthop Res 2011; 29: 547-555.

[24] O'Connell GD, Jacobs NT, Sen S, Vresilovic EJ and Elliott DM. Axial creep loading and unloaded recovery of the human intervertebral disc and the effect of degeneration. J Mech Behav Biomed Mater 2011; 4: 933-942.

[25] Fukuta S, Miyamoto K, Iwata A, Hosoe H, Iwata H, Shirahashi K and Shimizu K. Unusual back pain caused by intervertebral disc degeneration associated with schmorl node at Th11/12 in a young athlete, successfully treated by anterior interbody fusion: a case report. Spine (Phila Pa 1976) 2009; 34: E195-198.

[26] Wang L, Cui W, Kalala JP, Hoof TV and Liu BG. To investigate the effect of osteoporosis and intervertebral disc degeneration on the endplate cartilage injury in rats. Asian Pac J Trop Med 2014; 7: 796-800.

[27] Melrose J, Shu C, Young C, Ho R, Smith MM, Young AA, Smith SS, Gooden B, Dart A, Podadera J, Appleyard RC and Little CB. Mechanical destabilization induced by controlled annular incision of the intervertebral disc dysregulates metalloproteinase expression and induces disc degeneration. Spine (Phila Pa 1976) 2012; 37: 18-25.

[28] Zhang H, Yang S, Wang L, Park P, La Marca F, Hollister SJ and Lin CY. Time course investigation of intervertebral disc degeneration produced by needle-stab injury of the rat caudal spine: laboratory investigation. J Neurosurg Spine 2011; 15: 404-413.

[29] Zhang W, Li T, Gong Q, Shi R, Zhao X, Feng G, Wang B, Liu X and Liu H. [A comparative study on establishing rabbit intervertebral disc degeneration models by three methods]. Zhongguo Xiu Fu Chong Jian Wai Ke Za Zhi 2010; 24: 41-45.

[30] Nuckley DJ, Kramer PA, Del Rosario A, Fabro N, Baran S and Ching RP. Intervertebral disc degeneration in a naturally occurring primate model: radiographic and biomechanical evidence. J Orthop Res 2008; 26: 1283-1288.

[31] Sakai Y, Matsuyama Y, Hasegawa Y, Yoshihara H, Nakamura H, Katayama Y, Imagama S, Ito Z, Ishiguro N and Hamajima N. Association of gene polymorphisms with intervertebral disc

degeneration and vertebral osteophyte formation. Spine (Phila Pa 1976) 2007; 32: 1279-1286.

[32] Yu LP, Qian WW, Yin GY, Ren YX and Hu ZY. MRI assessment of lumbar intervertebral disc degeneration with lumbar degenerative disease using the Pfirrmann grading systems. PLoS One 2012; 7: e48074.

[33] Modic MT, Masaryk TJ, Ross JS and Carter JR. Imaging of degenerative disk disease. Radiology 1988; 168: 177-186.

[34] Pearce RH, Thompson JP, Bebault GM and Flak B. Magnetic resonance imaging reflects the chemical changes of aging degeneration in the human intervertebral disk. J Rheumatol Suppl 1991; 27: 42-43.

[35] Hughes SP, Freemont AJ, Hukins DW, McGregor AH and Roberts S. The pathogenesis of degeneration of the intervertebral disc and emerging therapies in the management of back pain. J Bone Joint Surg Br 2012; 94: 1298-1304.

[36] Huang M, Wang HQ, Zhang Q, Yan XD, Hao M and Luo ZJ. Alterations of ADAMTSs and TIMP-3 in human nucleus pulposus cells subjected to compressive load: Implications in the pathogenesis of human intervertebral disc degeneration. J Orthop Res 2012; 30: 267-273.

[37] Gopal D, Ho AL, Shah A and Chi JH. Molecular basis of intervertebral disc degeneration. Adv Exp Med Biol 2012; 760: 114-133.

[38] Colloca CJ, Gunzburg R, Freeman BJ, Szpalski M, Afifi M and Moore RJ. Biomechancial quantification of pathologic manipulable spinal lesions: an in vivo ovine model of spondylolysis and intervertebral disc degeneration. J Manipulative Physiol Ther 2012; 35: 354-366.

[39] Kim NK, Shin DA, Han IB, Yoo EH, Kim SH and Chung SS. The association of aggrecan gene polymorphism with the risk of intervertebral disc degeneration. Acta Neurochir (Wien) 2011; 153: 129-133.

[40] Kirzner Y, Marcolongo M and Bhatia SK. Advances in biomaterials for the treatment of intervertebral disc degeneration. J Long Term Eff Med Implants 2012; 22: 73-84.

[41] Turgut M, Yenisey C, Akyuz O, Ozsunar Y, Erkus M and Bicakci T. Correlation of serum trace elements and melatonin levels to radiological, biochemical, and histological assessment of degeneration in patients with intervertebral disc herniation. Biol Trace Elem Res 2006; 109: 123-134.

[42] Kang JD, Stefanovic-Racic M, McIntyre LA, Georgescu HI and Evans CH. Toward a biochemical understanding of human intervertebral disc degeneration and herniation. Contributions of nitric oxide, interleukins, prosta-

glandin E2, and matrix metalloproteinases. Spine (Phila Pa 1976) 1997; 22: 1065-1073.

[43] Yurube T, Takada T, Suzuki T, Kakutani K, Maeno K, Doita M, Kurosaka M and Nishida K. Rat tail static compression model mimics extracellular matrix metabolic imbalances of matrix metalloproteinases, aggrecanases, and tissue inhibitors of metalloproteinases in intervertebral disc degeneration. Arthritis Res Ther 2012; 14: R51.

[44] Levicoff EA, Kim JS, Sobajima S, Wallach CJ, Larson JW 3rd, Robbins PD, Xiao X, Juan L, Vadala G, Gilbertson LG and Kang JD. Safety assessment of intradiscal gene therapy II: effect of dosing and vector choice. Spine (Phila Pa 1976) 2008; 33: 1509-1516; discussion 1517.

[45] Kwon YJ. A minimally invasive rabbit model of progressive and reproducible disc degeneration confirmed by radiology, gene expression, and histology. J Korean Neurosurg Soc 2013; 53: 323-330.

[46] Gorth DJ, Mauck RL, Chiaro JA, Mohanraj B, Hebela NM, Dodge GR, Elliott DM and Smith LJ. IL-1ra delivered from poly(lactic-co-glycolic acid) microspheres attenuates IL-1beta-mediated degradation of nucleus pulposus in vitro. Arthritis Res Ther 2012; 14: R179.